Ionospheric behavior statistics from the Livingston station

Olga A. Maltseva, Tatyana V. Nikitenko
Institute for Physics, Southern Federal University, 344090, Rostov-on-Don, Russia, mal@ip.rsu.ru

Abstract

The existing statistics of the Antarctic ionosphere parameters behavior is supplemented by the results from the Livingston station data for the summer periods of 2005-2019, 35 months in total. The climatology of the parameters behavior came to the constancy of the values of the critical frequency foF2 in the local daytime and evening times and significant differences at night, reaching factor 2. The highest values are in December, the lowest in March. For the maximum height hmF2, the spread of values is small. A comparison of the values of foF2 and hmF2 of the IRI model with observational data is carried out. A certain tendency of an increase in deviations with an increase in solar activity was found. For foF2, dispersion σ does not exceed 25%, for hmF2 - 17%. The average values for the entire period are: |ΔfoF2|=0.73 MHz, σ(foF2) =0.86 MHz and 13.6%, |ΔhmF2| =22.5 km, σ(hmF2)=27.5 km and 9.65%. These magnitudes are close to those for stations in the northern hemisphere. The possibility of using the total electron content for determining foF2 is shown.

1 Introduction

Every year the prospects for the use of the Antarctic continent become more obvious, which leads to the intensification of its exploration. This fully applies to ionospheric research. Many papers emphasize the importance of knowing the state of the ionosphere in the Antarctic zone and using HF propagation (e.g. [1]). In the paper [2], a pilot project on oblique propagation of HF radio waves near the South Pole is described and it is noted that the success of this relatively inexpensive experiment indicates the possibility of deploying a stationary network of ionosondes for a comprehensive observational coverage of the Antarctic ionosphere. From the very beginning, studies of the ionosphere in Antarctica were focused on using the IRI model [3]; therefore, many papers were devoted to comparing observational data with model parameters, including for such a parameter as the total electron content TEC. For example, in the paper [4] the comparison was carried out on a large data set at the maximum (2000-2001) and minimum (2007-2008) solar activity. The data of vertical sounding at the San Martin station (68.1◦S, 293.0◦E) and the GPS receiver at Higgins were used. It is shown that the diurnal, seasonal dependences of foF2 and TEC and their dependence on solar activity are similar; in summer, daytime values are less than nighttime ones. The results of a comparison of the observational foF2 with the IRI model showed the correspondence of daily trends and the presence of periods when the model can both overestimate and underestimate the observational values. Particular attention is paid to the behavior of the Antarctic ionosphere during disturbances. Thus, in [5], foF2 data from four Antarctic stations were analyzed during three intense magnetic storms occurred in high solar activity (years 2002 and 2003) and the features of the behavior of this parameter were found both in the main phase of a magnetic storm and in the recovery phase. Since additional statistics are never superfluous, this paper presents the results of studying the behavior of the ionosphere from the Livingston station data. Climatological regularities are given, a comparison with the IRI model, the possibility of using TEC to determine foF2 is investigated.

2 Climatology of parameters foF2 and hmF2

Experimental data for Livingston Island station (lat: -62.4, lon: 300.5) were taken from the website (obsebre.es/en/Livingston-ionograms) from 2005 to 2019. Table 1 gives the observation periods during the expeditions for each year. There are 2 columns for the months with the most available data. A certain amount of data refers to December and March, but they did not fit into the table. 35 months in total.

Table 1. Basic data for Livingston station

Год	1	2
2005	3-19.02.2005	17-31.12.2005
2006	1-31.01.2006	1-20.02.2006
2007	24-31.01.2007	1-24.02.2007
2008	1-31.01.2008	1-21.02.2008
2009	11-25.12.2009	
2011	9-31.01.2011	9-31.01.2011
2012	1-31.01.2012	1-15.02.2012
2013	5-31.01.2013	1-17.02.2013
2014	24-31.01.2014	1-17.02.2014
2015	1-31.01.2015	1-20.02.2015
2016	1-31.01.2016	1-17.02.2016
2017	1-31.01.2017	1-28.02.2017
2018	6-31.01.2018	1-28.02.2018
2019	15-31.01.2019	1-28.02.2019

The diurnal and seasonal variations can be illustrated by one graph. The most complete period, including four months, is the end of 2016 and the beginning of 2017 (the summer season of minimum solar activity). The results are shown in Figure 1 for the local time LT. Inside the picture, next to the icon for a specific curve, there is a letter representing the month and year.

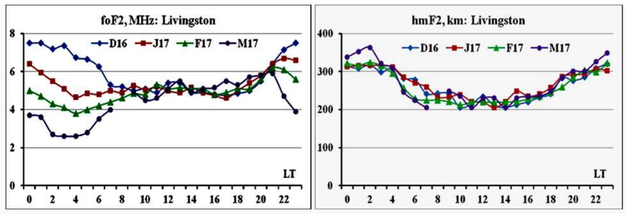

Figure 1. An example of the daily variation of ionospheric parameters at the Livingston station

For foF2, one can see the constancy of values in the daytime and in the evening, and significant differences at night, reaching factor 2. The highest values are in December, the lowest are in March. For hmF2, the spread of values is small and the curve averaged over four months can be approximated by a polynomial of the second degree hmF2 = $373.98 - 23.391 \cdot LT + 0.8952 \cdot LT^2$ with a confidence factor of 0.92. The rest of the cases include three months (December, January, February or January, February, March). For these cases in 2019 in conditions of low solar activity, the results are identical to those shown in Figure 1. In three months of 2011-2012, with a higher solar activity, the trends persist with higher values of foF2 and hmF2 than in Figure 1, and with a decrease in the period of constant foF2. In conditions of high solar activity, the differences between monthly medians decrease significantly (Figure 2).

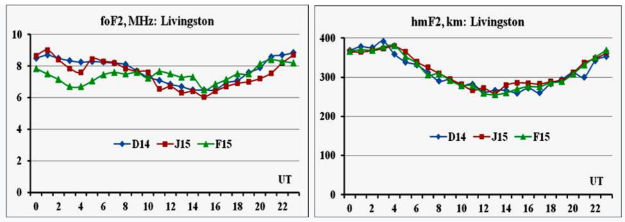

Figure 2. Daily variations in parameters under conditions of high solar activity

The dependence of the parameters foF2 and hmF2 on the F10.7 index is shown in Figure 3 for several UT hours using the example of January. For the parameters, medians are given, for the index - monthly averages. The correspondence between index values and years is shown in Table 2, along with the number of available parameter values for each year (third column).

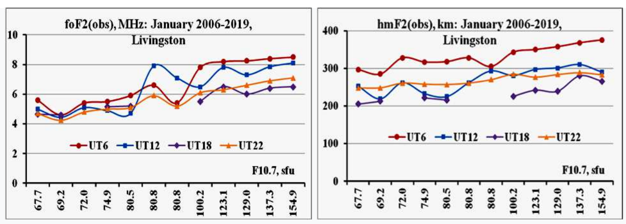

Figure 3. Dependence of the parameters foF2 and hmF2 on the F10.7 index

The same dependences are obtained for February.

Table 2. Statistics of observations by years

F10.7	Year	N
67.71	18	25
69.23	19	15
71.95	8	31
74.87	17	31
80.5	11	22
80.76	6	31
80.81	7	6
100.15	16	31
123.05	13	26
128.97	12	31
137.33	15	31
154.89	14	8

There is a certain trend in the increase in the values of the parameters with an increase in solar activity. One can also note that not all years have complete statistics and there are even cases when there is not a single measurement during the whole month. Figure 4 shows the dependence of the parameters foF2 and hmF2 of the IRI model on the F10.7 index for the same hours.

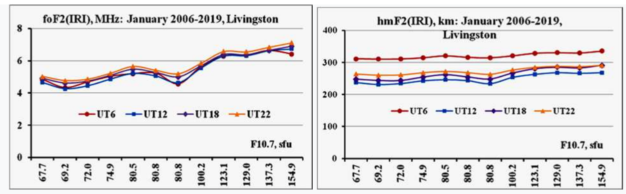

Figure 4. Dependence of the parameters foF2 and hmF2 of the IRI model on the F10.7 index

It can be seen that the model underestimates the values of both parameters and the scatter of values in the diurnal variation is not so large; nevertheless, the trend of dependence on solar activity exists to a greater extent for foF2 and to a lesser extent for hmF2. An illustration of the differences between the observational and model daily variations is given in Figure 5 for the months 2018 (minimum F10.7) and 2014 (maximum F10.7).

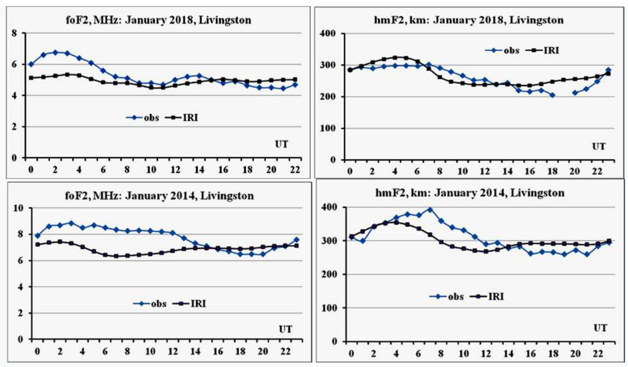

Figure 5. An example of comparing observational and model values of parameters

It can be seen that the largest deviations fall on the first half of the UT day and are greater at the solar maximum than at the minimum. The correspondence of foF2 and hmF2 values (model accuracy) was estimated for all available data using absolute and relative deviations |ΔfoF2|, σ(foF2), |hmF2|, σ(hmF2). Figure 6 shows the corresponding results depending on the solar activity index F10.7. The upper graphs show the absolute and relative deviations in the corresponding units of measurement, the lower ones - the relative deviations in %.

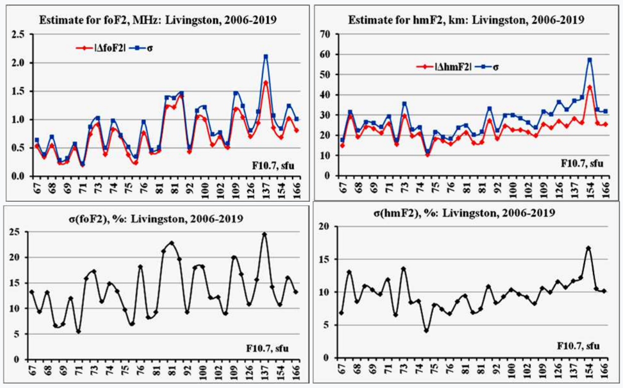

Figure 6. Statistical characteristics of the ionospheric parameters for the Livingston station

There is a certain tendency for the deviations to grow with increasing solar activity. For foF2, σ does not exceed 25%, for hmF2 - 17%. The average values for the entire period are: |ΔfoF2|=0.73 MHz, σ(foF2)=0.86 MHz and 13.6%, |ΔhmF2|=22.5 km, σ (hmF2)=27.5 km and 9.65%. These values are close to those for stations in the northern hemisphere.

3 Behavior during disturbances

The TEC parameter should play an important role in the study of the Antarctic ionosphere, as evidenced by a large number of publications, including comparisons with the IRI model (e.g. [6-7]). However, at the Livingston station, there were no TEC measurements and in this paper, the values of the global JPL map are used, calculated from the data of IONEX files (ftp://cddis.gsfc.nasa.gov/pub/gps/products/ionex/) with a step of 2 hours. The main attention was paid to the possibility of using the observational values TEC(obs) and the median of the equivalent ionospheric slab thickness τ(med) to determine foF2(rec), which showed itself well in the northern hemisphere [8]. Figure 7 provides confirmation of this possibility using the example of the strongest disturbance on January 1-5, 2016. The top panel shows the behavior of the Dst index, the lower left panel gives the behavior of TEC(obs) along with the median to illustrate the nature of the disturbances. The lower right panel compares the observational values foF2 (obs), the values foF2(rec) obtained by the combined use of TEC(obs) and τ(med), as well as the values of foF2(IRI) for the IRI model.

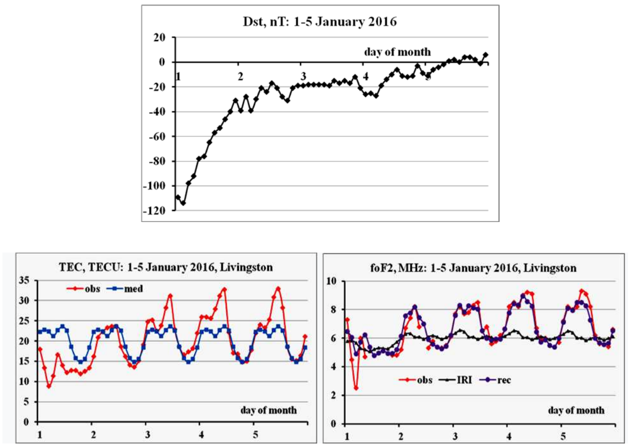

Figure 7. Illustration of the possibility of using TEC and τ(med) to determine foF2

It can be seen that at the beginning of the recovery phase a negative disturbance is observed, and at the end of the phase - a positive disturbance. This behavior is also observed at other stations in the southern hemisphere. The IRI model reflected the negative disturbance well, but provided only underestimated values on the remaining days. For almost all months considered, disturbed periods can be found, and the frequencies foF2(rec) were calculated for all cases. If to compare the absolute deviations |ΔfoF2| for foF2(IRI) and foF2(rec), then the average values of these quantities are 0.96 MHz and 0.57 MHz. The cases of the smallest and largest deviations in Figure 6 correspond to March 1-11, 2019 and December 20-31, 2011. The results for these cases are shown in Figure 8. Graphs are given for TEC, showing the presence of disturbances (deviations from the medians), and graphs for different foF2: observational foF2(obs), reconstructed foF2(rec) and model foF2(IRI).

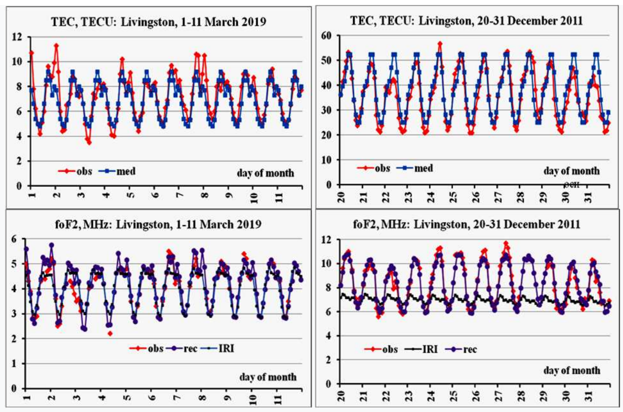

Figure 8. Behavior of ionospheric parameters for cases of limiting deviations of foF2

The corresponding absolute deviations in the first case are equal to |ΔfoF2(rec)|= 0.26 MHz and |ΔfoF2(IRI)|=0.3 MHz, in the second case |ΔfoF2(rec)|=0.41 MHz and |ΔfoF2(IRI)|=1.76 MHz. It can be seen that in the first case, both options provide a good match, but the model does not reflect the nature of the disturbance; in the second case, the values themselves are far from real.

4 Conclusion

The statistics of the parameters foF2 and hmF2 behaviour on the long-term data of the station Livingston is obtained. The insignificant trend of increase of values with growth of index F10.7 was revealed. In spite of the fact that modeling parameters of the ionosphere for the southern hemisphere station give conformity with observational data not worse, than parameters in the northern hemisphere, the obtained statistics confirms necessity of a network of ionosondes in the Antarctic region. It is confirmed also, that values of TEC can be used both for studying of disturbance nature, and for definition of foF2.

5 Acknowledgements

Authors thank the employees who have provided the data of the Livingston station. Authors express the gratitude to Community Coordinated Modeling Center for granting of model IRI online and to organizations and scientists providing data of JPL maps. The work was supported by the Ministry of Science and Higher Education of Russia (State assignment in the field of scientific activity, Southern Federal University, № 0852-2020-0015).

7 References

1. J. Porté, J. L. Pijoan, J. Masó, D. Badia, A. Zaballos, and R.M. Alsina-Pagès, "Advanced HF Communications for Remote Sensors in Antarctica," In: *Antarctica - A Key to Global Change*, 2018, pp. 1-19, DOI: http://dx.doi.org/10.5772/intechopen.81108.

2. A. T. Chartier, J. Vierinen, and G. Jee, "First observations of the McMurdo–South Pole oblique ionospheric HF channel,“ *Atmos. Meas. Tech*. **13**, 2020, pp. 3023–3031, https://doi.org/10.5194/amt-13-3023-2020.

3. D. Bilitza, D. Altadill, D. Truhlik, V. Shubin, I. Galkin, B. Reinisch, and X. Huang, "International Reference Ionosphere 2016: From ionospheric climate to real-time weather predictions," *Space Weather*, **15**, 2017, pp.418–429, doi: 10.1002/2016SW001593.

4. M. Mosert, L. A. McKinnell, M. Gende, C. Brunini, J. Araujo, R. G. Ezquer, and M. Cabrera, "Variations of foF2 and GPS total electron content over the Antarctic sector," *Earth Planets Space*, **63**, 2011, pp. 327–333, doi:10.5047/eps.2011.01.006.

5. G. A. Mansilla, "Response of the Antarctic Ionosphere to Some Intense Geomagnetic Storms," *The Open Atmospheric Science Journal*, **11**, 2017, pp. 16-28, DOI: 10.2174/1874282301711010016.

6. A. K. Gwal, P. Bhawre, A. A. Mansoori, and P. A. Khan, "Study of GPS Derived Total Electron Content and Scintillation Index Variations over Indian Arctic and Antarctic Stations," *J. Sci. Res*., **5(2)**, 2013, pp. 255-264, doi: http://dx.doi.org/10.3329/jsr.v5i2.12724.

7. P. Khatarkar, P. Bhawre, V. Kachneria, P. K. Purohit, and A. Gwal, "Behavior of Total Electron Content over auroral region at Maitri, Antarctica," *International Journal of Scientific & Engineering Research*, **5(9)**, 2014, pp. 1-7.

8. O. A. Maltseva, and N. S. Mozhaeva, "Empirical modeling of the total electron content of the ionosphere," In: *Empirical modelling and its applications*. - Edited by Mamun Habib. Chapter 1, 2016, pp. 1-28. ISBN 978-953-51-2494-8.